AMERICAN SOCIETY FOR MICROBIOLOGY | Journal of Virology®

VACCINES AND ANTIVIRAL AGENTS

Development of a Simian RNA Polymerase I Promoter-Driven Reverse Genetics System for the Rescue of Recombinant Rift Valley Fever Virus from Vero Cells

Tetsuro Ikegami[a,b,c]

[a]Department of Pathology, The University of Texas Medical Branch at Galveston, Galveston, Texas, USA
[b]Sealy Center for Vaccine Sciences, The University of Texas Medical Branch at Galveston, Galveston, Texas, USA
[c]Center for Biodefense and Emerging Infectious Diseases, The University of Texas Medical Branch at Galveston, Galveston, Texas, USA

ABSTRACT Rift Valley fever (RVF), which has been designated a priority disease by the World Health Organization (WHO), is one of the most pathogenic zoonotic diseases endemic to Africa and the Arabian Peninsula. Human vaccine preparation requires the use of appropriate cell substrates to support the efficient production of a seed vaccine with minimum concerns of tumorigenicity, oncogenicity, or adventitious agents. Vero cells, which were derived from the African green monkey kidney, represent one of the few mammalian cell lines that are used for vaccine manufacturing. This study demonstrates the rescue of RVF virus (RVFV) MP-12 infectious clones in Vero cells using plasmids encoding the *Macaca mulatta* RNA polymerase I promoter. Although Vero cells demonstrated an ~20% transfection efficiency, only 0.5% of transfected cells showed the replication of viral genomic RNA, supported by the coexpression of RVFV N and L helper proteins. RVFV infectious clones were detectable in the culture supernatants at approximately 4 to 9 days posttransfection, reaching maximum titers during the following 5 days. The reamplification of rescued recombinant MP-12 (rMP-12) in Vero cells led to an increase in the genetic subpopulations, affecting the viral phenotype via amino acid substitutions in the NSs gene, whereas rMP-12 reamplified in human diploid MRC-5 cells did not increase viral subpopulations with NSs gene mutations. The strategy in which RVFV infectious clones are rescued in Vero cells and then subsequently amplified in MRC-5 cells will support the vaccine seed lot systems of live-attenuated recombinant RVFV vaccines for human use.

IMPORTANCE RVF is a mosquito-transmitted, viral, zoonotic disease endemic to Africa and the Arabian Peninsula, and its spread outside the area of endemicity will potentially cause devastating economic damage and serious public health problems. Different from classical live-attenuated vaccines, live-attenuated recombinant vaccines allow rational improvement of vaccine production efficiency, protective efficacy, and vaccine safety via genetic engineering. This study demonstrated the generation of infectious Rift Valley fever (RVF) virus from cloned cDNA using Vero cells, which are one of a few mammalian cell lines used for vaccine manufacturing. Subsequent reamplification of virus clones in Vero cells unexpectedly increased viral subpopulations encoding unfavorable mutations, whereas viral reamplification in human diploid MRC-5 cells could minimize the emergence of such mutants. Rescue of recombinant RVFV from Vero cells and reamplification in MRC-5 cells will support the vaccine seed lot systems of live-attenuated recombinant RVFV vaccines for human use.

KEYWORDS Rift Valley fever virus, MP-12 vaccine, reverse genetics, Vero cells, RNA polymerase I, vaccine seed lot systems

Citation Ikegami T. 2021. Development of a simian RNA polymerase I promoter-driven reverse genetics system for the rescue of recombinant Rift Valley fever virus from Vero cells. J Virol 95:e02004-20. https://doi.org/10.1128/JVI.02004-20.

Editor Mark T. Heise, University of North Carolina at Chapel Hill

Copyright © 2021 American Society for Microbiology. All Rights Reserved.

Address correspondence to teikegam@utmb.edu.

Received 9 October 2020
Accepted 24 December 2020
Accepted manuscript posted online 13 January 2021
Published 10 March 2021

Outbreaks of emerging or reemerging viruses pose significant threats to global health. The World Health Organization (WHO) has designated several priority diseases that pose the most significant potential public health risks due to a lack of or insufficient countermeasures, including coronavirus disease 2019 (COVID-19), Crimean-Congo hemorrhagic fever, Ebola virus disease, Marburg virus disease, Lassa fever, Middle East respiratory syndrome (MERS), severe acute respiratory syndrome (SARS), Nipah- and henipaviral diseases, Zika virus disease, and Rift Valley fever (RVF). In addition to the development of rapid and accurate diagnostic measures, effective vaccines are essential for the long-term control of these diseases (1).

RVF is a mosquito-borne zoonotic viral disease affecting humans and ruminants. RVF virus (RVFV) causes a self-limiting biphasic febrile illness, while $<$8% of patients develop hemorrhagic fever, encephalitis, or retinitis with a 0.5 to 1.0% mortality rate (2–4). Sheep, goats, and cattle are highly susceptible to RVFV, which manifests as diseases characterized by high rates of spontaneous abortion and fetal malformation in sheep, cattle, and goats and lethal hepatitis in newborn lambs and goat kids (5). RVFV is a risk group 3 pathogen and classified as a category A priority pathogen by the NIAID/NIH in the United States and an overlap select agent by the U.S. Department of Health and Human Services (HHS) and the U.S. Department of Agriculture (USDA). RVF in animals is also listed as a disease that must be reported to the World Organization for Animal Health (OIE). RVFV belongs to the genus *Phlebovirus* of the family *Phenuiviridae*. The tripartite RNA genome is comprised of the large (L), medium (M), and small (S) segments. The L segment encodes the RNA-dependent RNA polymerase (L protein), while the M segment generates two glycoprotein precursors from the 1st or 2nd start codon, which can be cleaved into (i) the NSm, Gn, and Gc proteins or (ii) the 78-kDa proteins, respectively (6, 7). The RVFV virions incorporate the 78-kDa proteins in mosquito cells but not Vero cells (8). The 78-kDa protein plays a role in viral dissemination in vector mosquitoes (7, 9), while the nonstructural NSm protein inhibits apoptosis in infected mammalian cells (10, 11). The S segment encodes N and NSs in an ambisense manner. The nonstructural NSs protein is a major virulence factor for RVFV that promotes the posttranslational degradation of the cellular double-stranded RNA (dsRNA)-dependent protein kinase R (PKR) and the transcription factor (TF) IIH subunit p62 proteins (12–15). The NSs protein can thus cause the cessation of general transcription, including type I interferon (IFN) genes (16, 17).

RVFV consists of a single serotype, and the disease can be prevented by vaccination, as the virus is highly susceptible to neutralizing antibodies. Since the 1950s, a live-attenuated Smithburn vaccine has been widely used in Africa and the Arabian Peninsula for veterinary purposes, while another live-attenuated veterinary vaccine, clone 13, has been available in several African countries since 2010 (18, 19). Due to the sporadic nature of RVF outbreaks, many countries in areas of endemicity have not implemented the regular immunization of susceptible animals (19). Although no RVF vaccines are currently licensed for use in humans, a formalin-inactivated RVFV Entebbe strain (TSI-GSD-200, an investigational new drug in the United States) has been used for the vaccination of personnel at high risk of RVFV infection (e.g., laboratory or military workers) since 1986 (20). However, this candidate vaccine has been characterized as having poor immunogenicity, requiring a minimum of three doses to maintain a neutralizing antibody titer of 1:40 (21). Alternatively, a live-attenuated MP-12 candidate vaccine (TSI-GSD-223, an investigational new drug in the United States) has been developed using the MP-12 strain of RVFV, which was generated by chemical mutagenesis of the wild-type, pathogenic ZH548 strain and has been tested for safety and immunogenicity (22, 23). The MP-12 candidate vaccine was able to induce long-term protective immunity in human volunteers through a single intramuscular vaccination during phase 2 clinical trials (e.g., producing a neutralizing antibody titer of $\sim$1:500 or higher lasting for at least 1 year) (24). More recently, the Coalition for Epidemic Preparedness Innovations (CEPI) approved the evaluation of two novel RVF candidate vaccines to accelerate the development of an appropriate vaccine for human use. Notably, both of these new RVF candidate vaccines (25, 26) were

live-attenuated, recombinant RVFV strains that were generated via reverse genetics systems.

Reverse genetics is a technique used to manipulate the viral genome via cloned cDNA, which has previously been used as an effective tool for the rational design of attenuated virus strains for vaccine application (27). To rescue the infectious clones of negative-stranded RNA viruses (e.g., bunyaviruses, influenza viruses, arenaviruses, orthomyxoviruses, paramyxoviruses, rhabdoviruses, and bornaviruses), viral genomic RNA and helper N and L proteins must be expressed together in susceptible cells because viral genomic RNA cannot be used as a template for viral N or L protein synthesis due to the lack of cap structure at the 5′ end of complementary-sense (positive-sense) RNA. The N and L proteins are expressed in *trans* and play crucial roles in the initiation of viral genomic RNA replication in transfected cells. Interestingly, it was reported that infectious clones of several bunyaviruses, including Bunyamwera virus, La Crosse virus, Schmallenberg virus, Oropouche virus, and RVFV, could be rescued without the helper plasmids expressing N and L proteins, which was presumably explained by the low levels of expression of N and L proteins from plasmids encoding the complementary-sense genomic RNA (28–32). A few distinct systems have been reported to rescue RVFV infectious clones: (i) the T7 RNA polymerase-dependent reverse genetics system, using rodent cell lines such as BHK/T7-9 or BSR T7/5, which stably express T7 RNA polymerase (33, 34); (ii) the mouse RNA polymerase I-dependent reverse genetics system, which uses BHK/T7-9 cells (28); and (iii) the human RNA polymerase I-dependent reverse genetics system, using a coculture of 293T cells and BHK-21 cells (35). Although all of these reported systems have efficiently rescued recombinant RVFV, the resulting viruses were not readily applicable to human vaccine production due to the use of less characterized continuous cell lines from animal origins as the cell substrates (e.g., BHK-21 cells, BHK/T7-9 cells, or BSR T7/5 cells).

The continuous Vero cell line, which was derived from the kidney tissue of an adult African green monkey, was established in Japan in 1962 and subsequently transferred to the NIH, ATCC, and WHO (36). The WHO reference cell bank Vero 10-87 was established in 1990 after its extensive safety validation, including tumorigenicity and adventitious agents, which became available to manufacturers for vaccine production (37, 38). The direct recovery of recombinant RVFV from Vero cells will have significant advantages for human RVF vaccine development by reducing the time required for the safety qualification of uncharacterized cell substrates. Human RNA polymerase I-dependent reverse genetics systems have previously been used to recover influenza A virus infectious clones (39) and arenavirus (lymphocytic choriomeningitis virus and Junin virus Candid#1 strain) clones from Vero cells (40, 41), whereas the human T7 RNA polymerase-dependent reverse genetics system was used to rescue an Ebola virus infectious clone from Vero cells (42). Due to the species-specific nature of RNA polymerase I, the rRNA gene promoter sequence derived from Vero cells was also used to rescue an influenza A virus infectious clone (43). A common obstacle encountered when using Vero cells is low transfection efficiency, which might affect the success rate of virus rescue. The present study reports the development of an RNA polymerase I-driven reverse genetics system, using the rRNA gene promoter derived from *Macaca mulatta*, for the first successful rescue of an RVFV recombinant MP-12 (rMP-12) strain infectious clone directly from Vero cells. Moreover, this study also showed genetic changes in rMP-12 infectious clones during reamplification in Vero or MRC-5 cells. This technical advancement will facilitate the development of novel RVF candidate vaccines for human use.

RESULTS

Rational design of a promoter and terminator for an RVFV reverse genetics system using Vero cells. The ribosomal DNA (rDNA), which consists of the 5′ external transcribed spacer (ETS), 18S rRNA, internal transcribed spacer 1 (ITS1), 5.8S rRNA, ITS2, 28S rRNA, and 3′ ETS (Fig. 1A), is mapped onto human chromosomes 13, 14, 15, 21, and 22 (44). Each rDNA operon is flanked by the intergenic spacer (IGS). The precursor rRNA promoter is located immediately upstream of the 5′-ETS rDNA operon, which

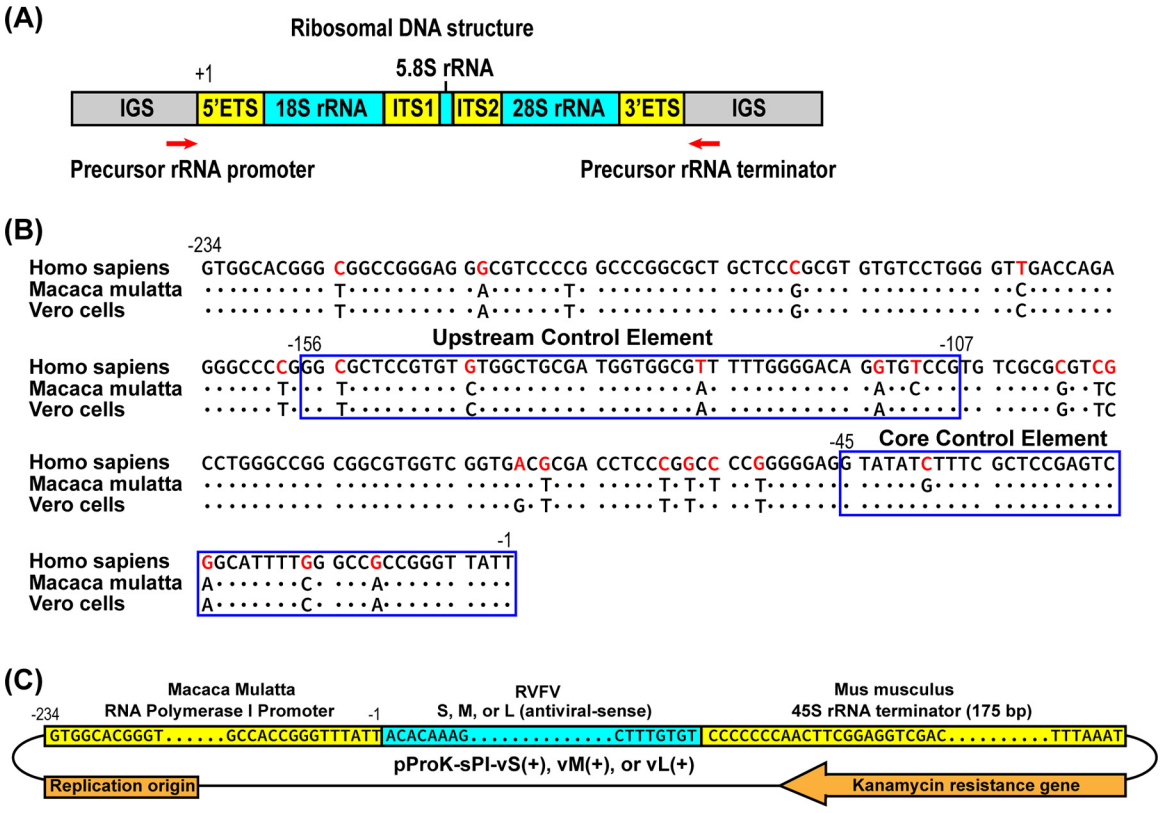

FIG 1 Use of the precursor rRNA promoter from *Macaca mulatta* in the reverse genetics system for Rift Valley fever virus. (A) Schematic representation of the repetitive units of ribosomal DNA (rDNA). The rDNA operon consists of the 5′ external transcribed spacer (ETS), 18S rRNA, internal transcribed spacer 1 (ITS1), 5.8S rRNA, ITS2, 28S rRNA, and 3′ ETS and is flanked by intergenic spacers (IGS). (B) Precursor rRNA promoter sequence (positions −234 to −1) alignment among *Homo sapiens* (chromosome 21; GenBank accession number NC_000021.9; positions 8388797 to 8389034), *Macaca mulatta* (chromosome 20; GenBank accession number NC_041773.1; positions 29808263 to 29808496), and Vero cells (GenBank accession number DI217998.1). The precursor rRNA promoter encodes two functional elements: (i) an upstream control element (UCE) (positions −156 to −107 relative to the transcription start site at position +1) and (ii) a core control element (CCE) (positions −45 to +18). (C) Schematic representation of plasmids encoding full-length antiviral-sense L, M, or S segments of RVFV, flanked by the precursor rRNA promoter (positions −234 to −1) of *Macaca mulatta* and the murine RNA polymerase I terminator.

encodes two important functional elements: (i) the upstream control element (UCE) (positions −156 to −107 relative to the transcription start site at position +1) and (ii) the core control element (CCE) (positions −45 to +18). The CCE is essential for the basal promoter activity of RNA polymerase I and determines the species specificity of the rRNA promoter (45, 46), whereas the presence of the UCE upstream of the CCE supports the maximum level of transcription. The far-upstream region (positions −234 to −167) can also strengthen transcription (47). A sequence alignment of the precursor rRNA promoter (positions −234 to −1) among *Homo sapiens*, *Macaca mulatta*, and Vero cells is shown in Fig. 1B. Between *Homo sapiens* and *Macaca mulatta*, 23 nucleotide (nt) differences were identified within the entire 234-nt region, 4 of which were located within the CCE. Between *Macaca mulatta* and Vero cells, only 4 nt differences were identified within the entire 234-nt region, 1 of which was located within the CCE. Based on the similarity between the rRNA promoter CCE sequences of *Macaca mulatta* and Vero cells, we constructed reverse genetics plasmids for RVFV using the precursor rRNA promoter (positions −234 to −1) of *Macaca mulatta* combined with a well-characterized murine RNA polymerase I terminator sequence (Fig. 1C).

Functional expression of RVFV genomic RNA and viral proteins in Vero cells. The transfection efficiency of Vero cells was then evaluated by using 0.6 μg of the pCAGGSK-vN or 0.5 μg of the pCAGGSK-vG plasmid. We adjusted the total plasmid

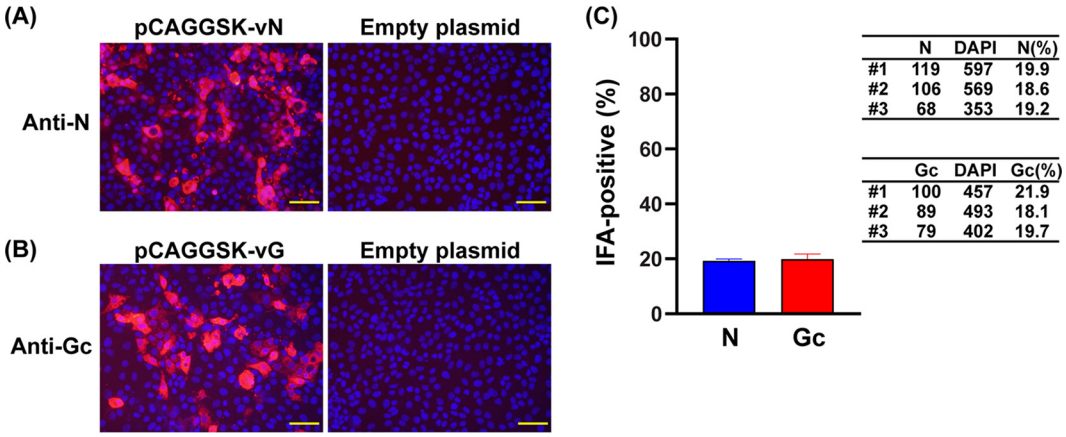

FIG 2 Expression of Rift Valley fever virus (RVFV) N or Gc proteins in transfected Vero cells. (A and B, left) Vero cells were transfected using 12 μl of TransIT-293 transfection reagent and 0.6 μg of the pCAGGSK-vN plasmid (A) or 0.5 μg of the pCAGGSK-vG plasmid (B), together with the empty pCAGGSK plasmid to adjust the total plasmid amount to 4.0 μg. (Right) As negative controls, Vero cells were transfected with 4.0 μg of the empty pCAGGSK plasmid. At 72 h posttransfection, fixed cells were stained with anti-RVFV N (A) or anti-RVFV Gc (B) antibodies, followed by secondary antibodies conjugated to Alexa Fluor 594. Nuclei were stained with DAPI (4′,6-diamidino-2-phenylindole). (C) Actual counts of Alexa Fluor 594 signal-positive cells and DAPI-positive cells and graph of the means ± standard deviations of the ratios between Alexa Fluor 594 signal-positive cells and DAPI-positive cells from three different images. Bars, 50.0 μm.

quantity to 4 μg using an empty plasmid and transfected 1×10^6 cells per well in a 6-well plate to maintain consistency throughout the reverse genetics experiment. As shown in Fig. 2, RVFV N and Gc proteins were abundantly expressed in approximately 19% to 20% of Vero cells.

Next, the RNA replication of the S-GFP genome, in which the NSs gene of the S segment was replaced with the green fluorescent protein (GFP) gene, was evaluated in transfected Vero cells. Although the S-GFP genome harbors the GFP gene, the GFP protein can be expressed only when GFP mRNA is transcribed from the S-GFP genome by the viral N and L proteins. To evaluate the background transfection efficiency, Vero cells were separately transfected with the EGFP-N1 plasmid, which can constitutively express GFP proteins. GFP expression from the EGFP-N1 plasmid was detected in 19% to 20% of cells, based on image analysis, whereas GFP expression from the S-GFP genome was detected much less frequently (Fig. 3A). Foci of GFP-positive cells were found; however, the evaluation of the numbers of GFP-positive cells unevenly scattered in wells was not realistic when performed by image analysis. Therefore, we resuspended transfected Vero cells at 72 h posttransfection (hpt) and evaluated the numbers of GFP- and DAPI (4′,6-diamidino-2-phenylindole)-positive cells using an automated cell counter. As shown in Fig. 3B, 18.3%, 0.47%, and 0% of Vero cells expressed EGFP-N1; S-GFP with N, L, and GnGc proteins; and S-GFP without N, L, and GnGc proteins, respectively, according to the detection of GFP signals.

To evaluate L, M, and S segment RNA replication in transfected Vero cells, we next performed Northern blot analysis of total RNA. Vero cells were mock transfected or cotransfected with pProK-sPI-vS(+), pProK-sPI-vM(+), pProK-sPI-vL(+), pCAGGSK-vN, pCAGGSK-vL, and pCAGGSK-vG (Fig. 3C). Without protein expression plasmids, only the positive-sense S segment RNA could be visualized, whereas the positive-sense M and L segments were too faint to be visualized. However, the accumulation of positive-sense L segment RNA could be detected in the presence of N protein. The coexpression of the N and L proteins, with or without GnGc proteins, led to the accumulation of negative-sense S and M segments, whereas the negative-sense L segment was still not detectable in the analysis. These results indicated that S segment RNA could be replicated more abundantly than M segment RNA in transfected Vero cells, whereas the replication of L segment RNA in transfected Vero cells was below the detection limit of the Northern blot analysis.

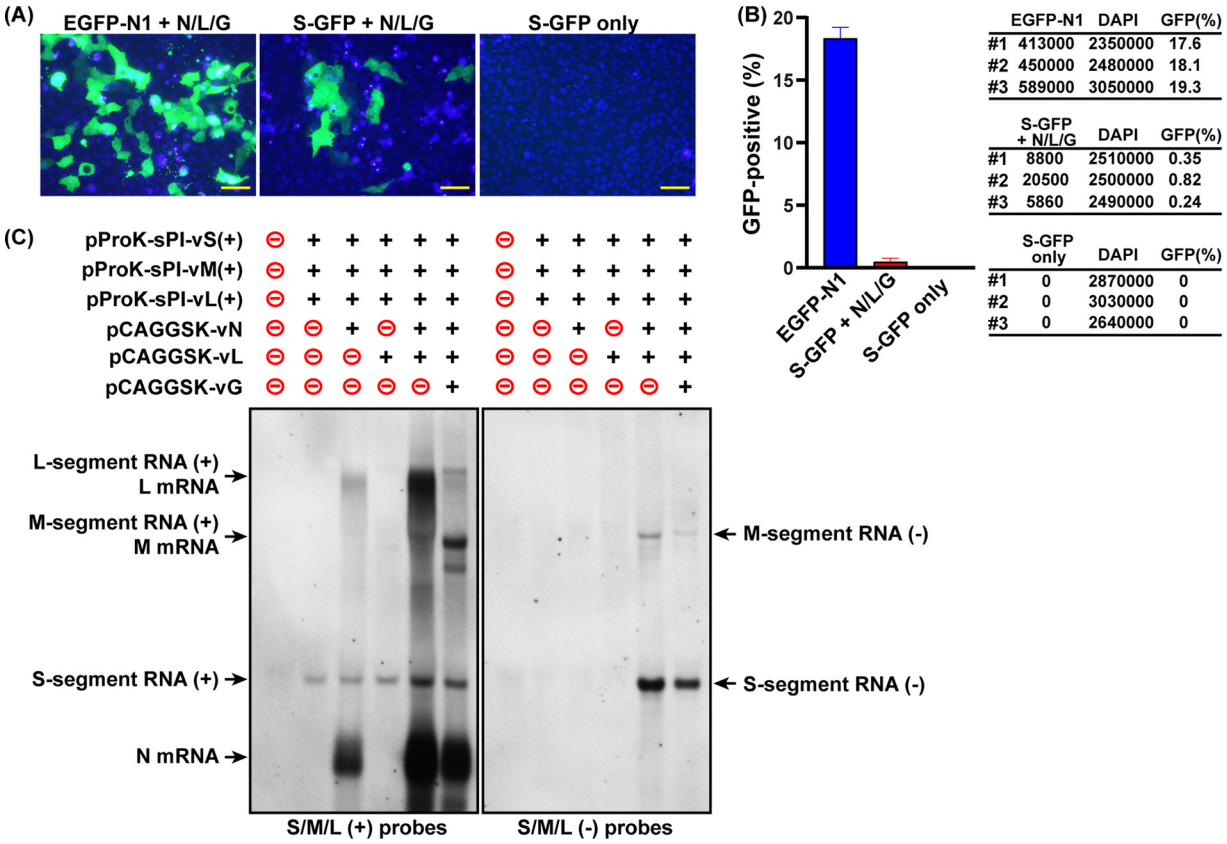

FIG 3 Analysis of RVFV S segment RNA replication in transfected Vero cells. (A) Vero cells in 6-well plates (1×10^6 cells/well) were transfected with 0.8 μg of pEGFP-N1 or pProK-sPI-vS(+)-GFP, together with 0.6 μg of pCAGGSK-vN, 0.5 μg of pCAGGSK-vL, 0.5 μg of pCAGGSK-vG, and 1.6 μg of pCAGGSK (empty) plasmids, using 12 μl of the TransIT-293 transfection reagent. As a control (S-GFP only), Vero cells were transfected with 0.8 μg of pProK-sPI-vS(+)-GFP and 3.2 μg of pCAGGSK (empty) plasmids. Images represent the expression of GFP at 72 h posttransfection. Nuclei of live cells were stained with DAPI. Bars, 50.0 μm. (B) The numbers of GFP- and DAPI-positive cells were measured by an automated cell counter. The actual counts of GFP-positive cells and DAPI-positive cells and a graph of the means ± standard deviations of the ratios between GFP-positive cells and DAPI-positive cells from three different wells are shown. (C) Vero cells were mock transfected or transfected with the indicated combinations of plasmids. At 72 h posttransfection, total RNA was collected and analyzed by Northern blotting using RNA probes to detect positive-sense L, M, and S segment RNAs (left) or negative-sense L, M, and S segment RNAs (right).

Rescue of the infectious recombinant MP-12 strain from cloned cDNA in Vero cells. The recovery of rMP-12 infectious clones was performed using Vero cells. Six different wells (wells 1 to 6) were separately transfected with a series of plasmids, i.e., pProK-sPI-vS(+), pProK-sPI-vM(+), pProK-sPI-vL(+), pCAGGSK-vN, pCAGGSK-vL, and pCAGGSK-vG. The virus titers in the culture supernatants and the appearance of a cytopathic effect (CPE) of cell rounding or detachment in the culture monolayer were analyzed daily up to 16 days posttransfection (dpt). Because the 6-well plate became 100% confluent by 72 hpt, the cells in each well were trypsinized and transferred to a 10-cm dish at 72 hpt. By 7 dpt, all plates showed 10 to 15 small plaque-like foci on monolayers. All foci disappeared in the following days in wells 1 and 3, and no infectious clones were detected at 16 dpt. In wells 2, 4, 5, and 6, a few foci increased in size, which eventually led to widespread CPE, characterized by the rounding or detachment of cells in the monolayer (Fig. 4A). In the culture supernatants, infectious rMP-12 could be detected as early as 4 dpt (well 5), whereas well 4 did not contain detectable rMP-12 by 9 dpt. Nevertheless, virus titers of rMP-12 reached 10^6 PFU/ml or higher at 12 dpt in the wells with successful rescue.

Subsequently, additional virus rescue attempts were made (experiments i to vi) to test the requirement of the pCAGGSK-vG plasmid (Fig. 4B). Vero cells were transfected with pProK-sPI-vS(+), pProK-sPI-vM(+), pProK-sPI-vL(+), pCAGGSK-vN, and pCAGGSK-vL.

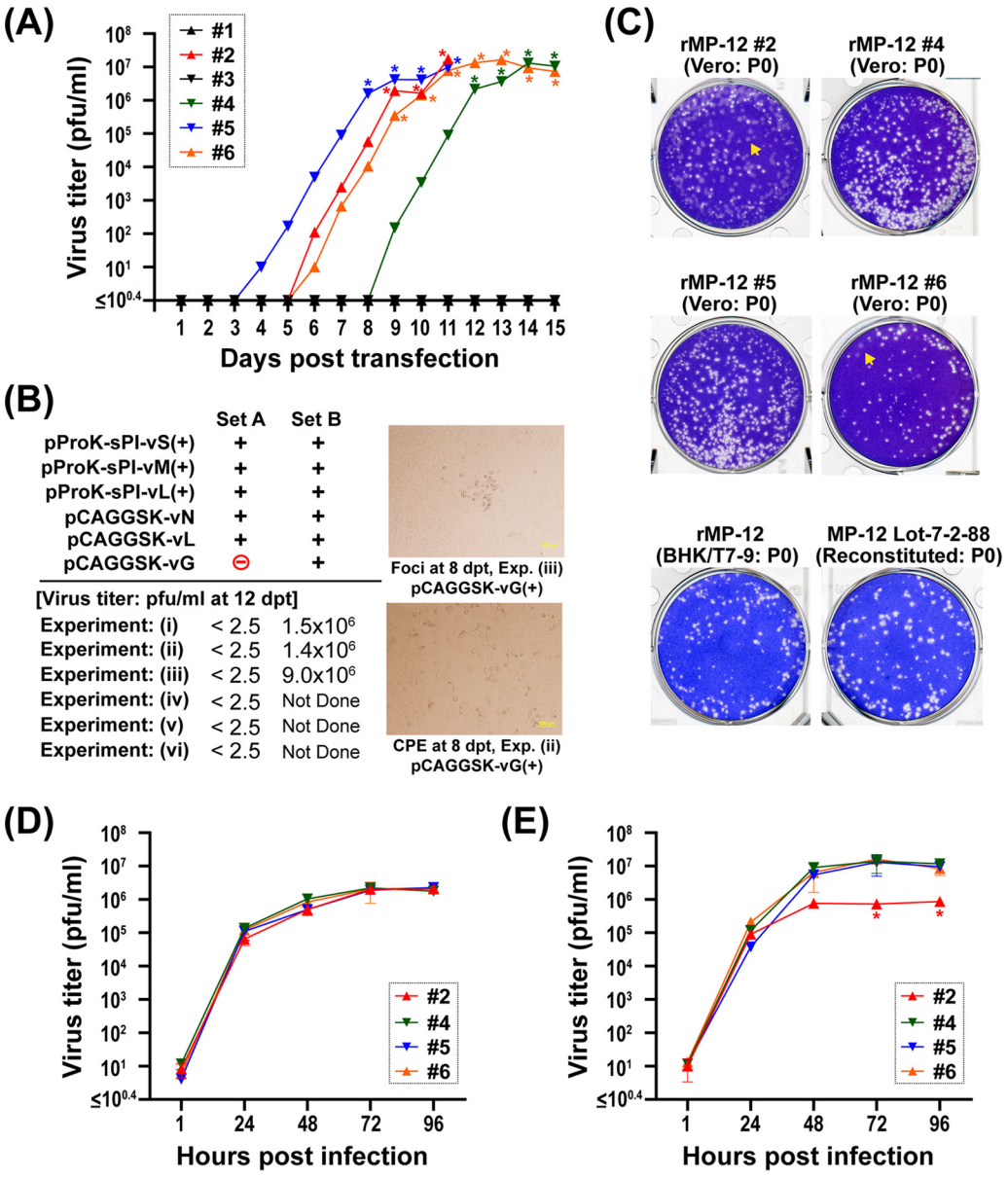

FIG 4 Rescue of rMP-12 infectious clones from Vero cells. The recovery of RVFV rMP-12 strain infectious clones was performed using Vero cells. (A) Six different wells (wells 1 to 6) in the 6-well plate were separately transfected with pProK-sPI-vS(+), pProK-sPI-vM(+), pProK-sPI-vL(+), pCAGGSK-vN, pCAGGSK-vL, and pCAGGSK-vG. Virus titers in the culture supernatants and the appearance of the cytopathic effect (CPE) widespread in monolayers (asterisks) for 15 days posttransfection (dpt) are shown in a graph. Transfected cells were transferred to a 10-cm dish at 72 h posttransfection. (B) Virus titers in the culture supernatants of transfected Vero cells at 12 dpt (set A, $n = 6$; set B, $n = 3$). Set A used the empty pCAGGSK plasmid instead of pCAGGSK-vG, while set B included all plasmids. Disruptions of the monolayer (foci, detachment, or rounding) are also shown in the right panels. (C) Plaque phenotypes of rMP-12 infectious clones 2, 4, 5, and 6, which were collected at 7, 11, 7, and 8 dpt, respectively. Arrows indicate turbid plaques. For comparison, the plaque phenotypes of rMP-12 collected from transfected BHK/T7-9 cells at 4 dpt and MP-12 vaccine lot 7-2-88 are shown. (D and E) Viral replication kinetics of rMP-12 infectious clones 2, 4, 5, and 6 (passage 0 [P0]) at 35°C in Vero cells (D) and MRC-5 cells (E) (MOI of 0.01). Arithmetic means of $\log_{10}$ values were analyzed by one-way analysis of variance (ANOVA), followed by Tukey's multiple-comparison test. Asterisks represent statistical differences (*, $P < 0.001$ [versus clones 4, 5, and 6]).

The total plasmid quantity was adjusted to 4 μg using an empty plasmid. Without the pCAGGSK-vG plasmid (set A), Vero cells did not show detectable foci or virus-induced CPE for 20 days, while the virus titers of the culture supernatants collected at 12 dpt were below the detection limit (<2.5 PFU/ml). Along with this experiment, three additional

wells were tested with the full set of plasmids, including pCAGGSK-vG (set B). All three wells showed multiple foci or cell detachment or rounding by 8 dpt, while the virus titers in the culture supernatants were 1.4×10^6 to 9.0×10^6 PFU/ml at 12 dpt.

Next, the plaque phenotypes of rMP-12 virus rescued from Vero cells (wells 2, 4, 5, and 6) were compared to those from BHK/T7-9 cells (4 dpt, with no additional passages) or an authentic MP-12 vaccine (lot 7-2-88, with no additional passages) (Fig. 4C). rMP-12 collected from well 2 (7 dpt) and well 6 (8 dpt) contained turbid plaques in 61% and 9%, respectively, whereas rMP-12 collected from well 4 (11 dpt) or well 5 (7 dpt), rMP-12 collected at 4 dpt from BHK/T7-9 cells, or the reconstituted MP-12 vaccine lot 7-2-88 did not show detectable turbid plaques.

The MP-12 strain lacking a functional NSs gene has previously been shown to form turbid plaques in Vero cells (33). Since the NSs protein plays a major role in counteracting host innate immune responses (48, 49), we next analyzed the replication kinetics of rMP-12 infectious clones 2, 4, 5, and 6 (passage 0) in type I IFN-incompetent Vero cells or type I IFN-competent MRC-5 cells (Fig. 4D and E). Since the RVFV MP-12 strain has a weak temperature-sensitive phenotype (50, 51), viral amplification was performed at 35°C, except for virus adsorption for 1 h at 37°C. Although all clones replicated similarly in Vero cells, clone 2 did not efficiently replicate in MRC-5 cells compared to clone 4, 5, or 6. These results indicated that there are genetic variations among rMP-12 infectious clones derived from Vero cells.

Next-generation sequencing of rMP-12 infectious clones passaged in Vero or MRC-5 cells. The emergence of undesirable genetic subpopulations in vaccine seeds must be characterized. To explore a strategy designed to reduce genetic variations in infectious clones, each clone was reamplified at 35°C in Vero or MRC-5 cells at a low multiplicity of infection (MOI) (Fig. 5A). Although most clones were amplified to $\geq 1 \times 10^6$ PFU/ml in Vero or MRC-5 cells at 96 h postinfection (hpi), clone 2 failed to efficiently amplify in MRC-5 cells. Clone 2 in MRC-5 cells was therefore collected at 168 hpi, after the replacement of the culture supernatant at 96 hpi. Subsequently, fresh Vero or MRC-5 cells were infected with passage 1 viral stocks derived from Vero or MRC-5 cells, respectively, for their reamplification at 35°C. Total RNA was collected from infected Vero or MRC-5 cells at 48 hpi for viral transcriptome sequencing (RNA-Seq) analysis. The RNA-Seq results showed that rMP-12 infectious clones 2, 4, 5, and 6 amplified in Vero cells revealed 6, 4, 4, and 8 mutation sites with ≥1% variant detection, respectively, whereas those amplified in MRC-5 cells had 3, 6, 4, and 16 mutation sites with ≥1% variant detection, respectively. Figure 5B to D show the specific mutations for each clone in the L, M, and S segments, respectively. No overlapping mutation sites were observed among clones 2, 4, 5, and 6 except for a silent mutation in the M segment (C1307U) in clones 2 and 4. Moreover, no overlapping mutation sites were observed between clones amplified in Vero cells and the same clones amplified in MRC-5 cells except for L-P329S (C1003U) in clone 6, Gn-L600S (U1819C) in clone 5, and the N open reading frame (ORF) silent mutation C555U in clone 6. These results indicated that the overall pattern of genetic subpopulations was unique to each infectious clone. Amino acid changes that occurred in ≥5% of the genetic subpopulation were found in clones amplified in Vero cells, including the following: L155P in NSs (clone 2; 85%), S101T in the NSm/78-kDa protein (clone 2; 25%), E49K in the NSm/78-kDa protein (clone 4; 11%), and E393G in Gn (clone 5; 9%). None of the infectious clones amplified in MRC-5 cells showed amino acid substitutions that affected ≥5% of the genetic subpopulation. These results indicated that MRC-5 cells are more suitable than Vero cells for preventing the selection of rMP-12 genetic variants featuring amino acid substitutions.

DISCUSSION

This study demonstrated the recovery of RVFV infectious clones from cloned cDNA using Vero cells. The reverse genetics system for RVFV was developed in the 2000s, using BHK cells expressing T7 RNA polymerase (e.g., BHK/T7-9 and BSR T7/5) (33, 34). Later, the mouse RNA polymerase I-dependent reverse genetics system in BHK/T7-9 cells (28) and the human RNA polymerase I-dependent reverse genetics system in a

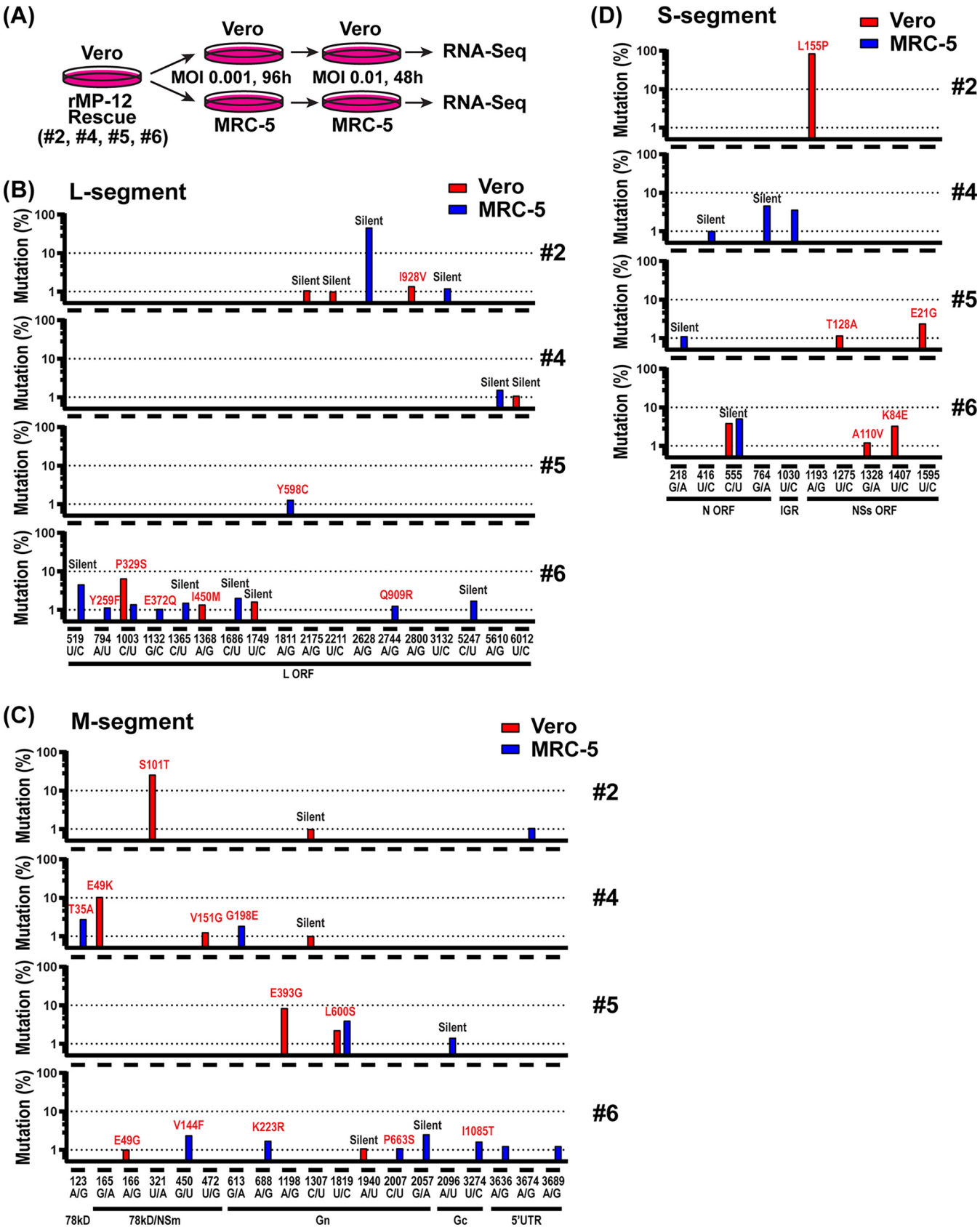

FIG 5 RNA-Seq analysis of rMP-12 infectious clones. rMP-12 infectious clones 2, 3, 5, and 6 were amplified twice, in either Vero or MRC-5 cells, at 35°C. Total RNA was analyzed by RNA-Seq. (A) Schematic representation of virus amplification methods in Vero or MRC-5 cells. (B to D) Graphs showing the detection of genetic variants (≥1%) in the L segment (B), the M segment (C), and the S segment (D) of infectious clones 2, 4, 5, and 6. The FASTQ reads were aligned with the L, M, or S segment sequences of the RVFV MP-12 strain (GenBank accession numbers DQ375404.1, DQ380208.1, and DQ380154.1).

coculture of 293T cells and BHK-21 cells (35) were reported. A potential pitfall of these reverse genetics systems was that BHK cells have never been used as cell substrates for live-attenuated vaccines intended for human use. Although most continuous cell lines are useful for research experiments, extensive validations of the safety of the proposed master and working cell banks will be required due to their inconsistent cellular conditions in terms of the passage number, the presence of adventitious agents, or potential tumorigenicity. Due to stringent safety requirements, only a limited number of mammalian cell substrates have been qualified for human vaccine production: (i) Wistar Institute 38 (WI-38) cells (human fetal diploid lung cells), which are used for the rabies virus vaccine, human adenovirus vaccine, and rubella virus vaccine; (ii) MRC-5 cells (human fetal diploid lung fibroblast cells), which are used for the rubella virus vaccine and varicella-zoster virus vaccine; (iii) FRhL-2 (fetal rhesus diploid lung) cells, which are used for the rotavirus vaccine; and (iv) Vero cells (continuous nonhuman primate cell line), which are used for the rotavirus vaccine, oral poliovirus vaccine, and smallpox vaccine (52, 53). Diploid cells such as MRC-5, WI-38, and FRhL-2 cells can respond to the stimulation of liposome-DNA complexes during DNA transfection, which may trigger type I interferon (IFN) responses, whereas Vero cells, which harbor deletions in the *IFNA* and *IFNB* genes on chromosome 15 (54), are less capable of inhibiting the expression or replication of viral RNA transcribed from the exogenous DNA templates and are more suitable for the successful recovery of RVFV infectious clones. The use of Vero cells in vaccine manufacturing is gaining acceptance from licensing authorities through the demonstrated safety of master or working Vero cell banks derived from the WHO Vero reference cell bank 10-87 (37). Validation of the removal of cellular DNA (10 ng per single human dose) is, however, one of the major regulatory requirements for viral vaccines derived from Vero cells (38). This study showed that infectious clones derived from Vero cells might contain genetic subpopulations that encode mutations in the 78-kDa/NSm genes, the NSs gene, or other structural genes. Therefore, the genetic characterization of the seed vaccine will be necessary prior to further large-scale viral amplification. Because the NSs mutants can efficiently replicate in type I IFN-incompetent Vero cells, the use of type I IFN-competent MRC-5 cells should reduce the replication of unfavorable NSs mutants in the vaccine stock. Viral propagation in MRC-5 cells will thus support the genetic stability of the MP-12 strain carrying the NSs gene.

In contrast to the reverse genetics systems in BHK cells, the efficiency of the rescue of RVFV from Vero cells was not high. In these rescue experiments, only a few foci of increasing size appeared after several days posttransfection, whereas many visible plaque-like foci disappeared from the monolayer within 1 week, likely because these plaque-like foci lacked the replication of L, M, or S segments. The transfection efficiency of Vero cells was measured to be approximately 20%, whereas the replication of the S segment was detected in 0.5% of the Vero cell monolayer. These results indicated that approximately 5,000 to 10,000 cells per well could support the replication of S segment RNA alone. Therefore, when all of the L, M, and S segments were combined, the number of cells able to support the replication of all three segments was likely even lower. A similar rescue efficiency was reported for a reverse genetics system for arenavirus using Vero cells, for which the viral genome is comprised of two RNA segments (41). To improve this low rescue efficiency in Vero cells, eight RNA polymerase I transcription cassettes were combined into a single plasmid to improve the efficiency of rescue of influenza A virus infection clones (39). Further reductions in plasmid variations are likely to support the more efficient rescue of RVFV infectious clones. It was also noted that plaque-like foci were not formed when Vero cells were transfected with a set of plasmids lacking pCAGGSK-vG. Northern blot analysis showed that the helper pCAGGSK-vG plasmid was dispensable for viral RNA replication in transfected Vero cells. It is possible that abundant expression of RVFV Gn and Gc proteins from the pCAGGSK-vG plasmid could support the production of infectious virus-like particles containing L, M, and/or S segments, which might facilitate the broad distribution of

viral RNA segments in Vero cells that might not have a full set of viral genomic RNA due to the poor transfection efficiency.

In this study, transfected Vero cells were transferred into 10-cm dishes at 72 hpt to prevent overconfluent conditions in the 6-well plates. We separately performed the same experiment twice ($n = 3$ each) without transferring transfected Vero cells into 10-cm dishes at 72 hpt. All wells showed plaque-like foci, which disappeared after 7 dpt. In both experiments, one out of three transfected wells demonstrated foci that increased in size, in which the rMP-12 virus titers of culture supernatants reached 4.5×10^3 PFU/ml and 1×10^7 PFU/ml, respectively, at 11 and 16 dpt. These results indicated that the transfer of transfected cells to a larger plate at 72 hpt is not essential for the rescue of rMP-12 infectious clones, although the rescue efficiency might be affected due to overconfluence.

This study used the RNA polymerase I promoter from *Macaca mulatta* chromosome 20 to transcribe the full-length L, M, and S segments of RVFV in Vero cells. The CCE of the promoter sequence determines the species specificity (45, 46), and the CCE sequences found in Vero cells and *Macaca mulatta* were nearly identical. CCE sequences have been reported to be highly conserved among *Pan troglodytes* (chimpanzee), *Gorilla gorilla* (gorilla), *Pongo abelii* (orangutan), *Nomascus leucogenys* (gibbon), and *Macaca mulatta* (rhesus macaque) (55). The CCE sequence similarity for the RNA polymerase I promoters between *Homo sapiens* (chromosome 21; GenBank accession number NC_000021.9; positions 8388797 to 8389034) and *Macaca mulatta* (chromosome 20; GenBank accession number NC_041773.1; position 29808263 to 29808496) was 91.1%. The *Homo sapiens* RNA polymerase I promoter can support the functional transcription of viral genomic RNA in Vero cells (39, 41), although the quantitative differences in promoter strength between simian and human RNA polymerase I promoters in Vero cells remain unknown. The correct termination site for human and nonhuman primate RNA polymerase I transcription has also not been functionally characterized. Transcription by murine RNA polymerase I can be terminated immediately upstream of a long C tract located upstream of a conserved SalI box, 5′-AGGTCGACCAG(T/A)(A/T)NTCCG-3′ (the SalI site is underlined) (56, 57). This murine RNA polymerase I terminator sequence has been shown to be functional in Vero cells (40, 41, 43). Thus, this study used the murine RNA polymerase I terminator sequence for the synthesis of viral genomic RNA with correct 3′ ends.

Despite the potential contribution to the virulence phenotype, the strong immunogenicity of the live-attenuated MP-12 candidate vaccine requires the NSs gene (58). The MP-12 strain encodes 23 point mutations in the L, M, and S segments, among which 2 amino acid substitutions in Gn (Y259H) and Gc (R1182G) in the M segment independently support attenuation (59), while 6 MP-12 mutations (78 kDa-I9T, 78 kDa-V17I, Gc-I747L, M-5′ UTR [untranslated region]-A3621G, L-G4368U, and L-5208G) were found in the genetic subpopulations of the parental pathogenic ZH548 strain (60). Amino acid substitutions in the L segment (L-V172A and L-M1244I) and the M segment (Gn-Y259H and Gc-R1182G) restrict viral replication at higher temperatures (50). The combination of several mutations in the MP-12 strain can thus contribute to the attenuation phenotype. In vaccinated animals or humans, the MP-12 strain can induce transient viremia below 10^3 PFU/ml (23). The original MP-12 vaccine has been extensively characterized for immunogenicity and safety since the 1980s and underwent a phase 2 clinical trial (20, 24). The NSs gene likely supports the low-level production of infectious virus particles, which in turn stimulates the production of neutralizing antibodies against RVFV via a single dose. Serial passage of MP-12 or the genetic variant in Vero or MRC-5 cells revealed an increase of reversion to wild-type sequences in Gc-R1182G, L-V172A, or L-M1244I at the subpopulation level (51). To further strengthen the attenuation of the MP-12 strain without abolishing immunogenicity, we are currently studying next-generation MP-12-based vaccines by using infectious clones obtained from Vero cells. Various live-attenuated candidate RVF vaccines, derived from the reverse genetics systems using BHK-derived cells, are currently being studied for human use by other laboratories, whereas little information is available regarding their

genetic stability during propagation in cell substrates. The overall strategy of rescuing RVFV infectious clones in Vero cells, followed by subsequent amplification in cell substrates optimal for genetic stability and regulatory clearance, will support the fundamental development of a rationally designed, live-attenuated RVFV vaccine for human use.

MATERIALS AND METHODS

Media, cells, and viruses. Vero cells (kidney epithelial cells, *Chlorocebus* sp.; ATCC CCL-81) or MRC-5 cells (human lung diploid cells; ATCC CCL-171) were maintained in Dulbecco's modified Eagle medium (DMEM) (Gibco, Thermo Fisher Scientific Inc., Waltham MA), containing 10% fetal bovine serum (FBS) (HyClone; GE Healthcare, Chicago, IL), penicillin (100 U/ml) (Gibco), and streptomycin (100 μg/ml) (Gibco), in a humidified cell culture incubator (5% CO_2 at 37°C). Baby hamster kidney cells that stably express T7 RNA polymerase (BHK/T7-9 cells) (61) were maintained in minimum essential medium alpha containing 10% FBS, penicillin (100 U/ml), streptomycin (100 μg/ml), and hygromycin B (600 μg/ml) at 37°C with 5% CO_2. The Vero, MRC-5, and BHK/T7-9 cells used in this study were verified to be mycoplasma free at The University of Texas Medical Branch at Galveston (UTMB) Tissue Culture Core Facility, and the identities of MRC-5 cells were authenticated by short tandem repeat analysis (UTMB Molecular Genomics Core Facility). Infectious clones of the rMP-12 strain were generated from cloned cDNA in Vero or BHK/T7-9 cells in this study. The MP-12 vaccine lot 7-2-88 was obtained from John C. Morrill (UTMB). Replications of the RVFV MP-12 and rMP-12 strains are restricted at temperatures above 38°C due to four temperature-sensitive mutations: Gn-Y259H (U795C), Gc-R1182G (A3564G), L-V172A (U533C), and L-M1244I (G3750A) (50, 51). To minimize the influence of temperature-sensitive mutations at 37°C (51), viral amplification was performed at 35°C, except for virus adsorption for 1 h at 37°C. The titration of the rMP-12 strain was performed at 37°C by a plaque assay using Vero cells with crystal violet staining (59) because the measurement of the plaque number was not affected at 37°C. The rescue of the rMP-12 strain from Vero cells was performed at 37°C to maintain physiologically optimal conditions for Vero cells.

Plasmids. The complementary-sense (positive-sense) pProT7-avS(+), pProT7-avM(+), and pProT7-avL(+) plasmids, which encode the full-length antiviral-sense S, M, and L segments of the RVFV MP-12 strain, respectively, immediately downstream of the T7 promoter, were described previously (59). For further vaccine development, these plasmids were modified by replacing the T7 promoter with the precursor rRNA gene promoter (positions −234 to −1) derived from *Macaca mulatta* chromosome 20 (GenBank accession number NC_041773.1; positions 29808263 to 29808496) and replacing the hepatitis delta virus ribozyme and T7 terminator sequences with the precursor rRNA gene terminator derived from *Mus musculus* (GenBank accession number X82564.1; positions 19042 to 19216). The gene fragments were synthesized using the gBlocks gene fragment synthesis service (Integrated DNA Technologies Inc., Coralville, IA). The ampicillin resistance gene was replaced with a kanamycin resistance gene due to increasing restrictions on the use of beta-lactam antibiotics in manufacturing areas [e.g., Article 21 CFR 211.42(d), 46(d), or 176 (65)]. The resulting plasmids were designated pProK-sPI-vS(+), pProK-sPI-vM(+), and pProK-sPI-vL(+). Additionally, the NSs gene of the MP-12 S segment was replaced with the green fluorescent protein (GFP) gene in the pProK-sPI-vS(+) plasmid, which was designated pProK-sPI(+)-GFP. The open reading frames of N, L, and glycoprotein precursor genes from the RVFV MP-12 strain were cloned downstream of the cytomegalovirus early enhancer and chicken β-actin promoter in a modified pCAGGS plasmid (pCAGGSK plasmid), in which the ampicillin resistance gene was replaced with a kanamycin resistance gene. The resulting plasmids were designated pCAGGSK-vN, pCAGGSK-vL, and pCAGGSK-vG.

Transfection of Vero cells. Vero cells grown in 10-cm dishes were trypsinized, and the number of cells was counted using a Countess II automated cell counter (Thermo Fisher Scientific). Next, 1×10^6 cells were placed into each well of a 6-well plate and allowed to spread in an incubator (1.5 ml medium per well with 5% CO_2 at 37°C under humidified conditions) for 40 to 50 min before transfection. Transfection was performed using a mixture containing 4 μg of plasmids and 12 μl of the TransIT-293 transfection reagent (Mirus Bio LLC, Madison, WI). Briefly, the transfection reagent was mixed with 150 μl Opti-MEM reduced serum medium (Gibco) and incubated for 5 min at room temperature. This mixture was added dropwise to the plasmid DNA and then incubated for 20 to 25 min at room temperature before being added to the 6-well culture. At 24 h posttransfection (hpt), the culture supernatant was replaced with fresh DMEM supplemented with 10% FBS and antibiotics.

Indirect fluorescence assay. Vero cells in 6-well plates (1×10^6 cells/well) were transfected with one of the following combinations, using 12 μl TransIT-293 transfection reagent: (i) 0.6 μg of plasmid pCAGGSK-vN and 3.4 μg of pCAGGSK (empty), (ii) 0.5 μg of pCAGGSK-vG and 3.5 μg of pCAGGSK (empty), or (iii) 4.0 μg of pCAGGSK (empty). At 72 hpt, the cells were fixed with methanol for 20 min at room temperature. Dried cells were hydrated with phosphate-buffered saline (PBS) and then blocked with PBS containing 0.5% bovine serum albumin (BSA) at 37°C for 1 h. Cells were then incubated with a 1:800 dilution of anti-RVFV N rabbit polyclonal antibody (63) or a 1:400 dilution of anti-RVFV Gc mouse monoclonal antibody (5G2), followed by 1:800 dilutions of either Alexa Fluor 594 goat anti-rabbit IgG (H+L) or Alexa Fluor 594 goat anti-mouse IgG(H+L), respectively, for the detection of specific signals. DNA was stained with 4′,6-diamidino-2-phenylindole (DAPI) (Thermo Fisher Scientific Inc.). Stained cells were then observed under an Olympus IX71 microscope with a DP71 camera (Olympus America, Center Valley, PA). Indirect fluorescence assay (IFA) images were incorporated by using DP manager software.

The numbers of DAPI- and Alexa Fluor 594 signal-positive cells were counted using the multipoint tool in ImageJ software (NIH) using three different images (64).

S segment reporter assay. To evaluate the transfection efficiency of Vero cells and the frequency of RVFV S segment RNA replication in transfected cells, Vero cells in 6-well plates (1×10^6 cells/well) were transfected with 0.8 μg of either plasmid pProK-sPI-vS(+)-GFP or pEGFP-N1 (TaKaRa Bio USA Inc., Mountain View, CA), 0.6 μg of pCAGGSK-vN, 0.5 μg of pCAGGSK-vL, 0.5 μg of pCAGGSK-vG, and 1.6 μg of pCAGGSK (empty), using 12 μl of the TransIT-293 transfection reagent. The negative-control wells were transfected with 0.8 μg of plasmid pProK-sPI-vS(+)-GFP and 3.2 μg of pCAGGSK (empty), using 12 μl of the TransIT-293 transfection reagent. At 72 hpt, the cells were stained with 10 μg/ml DAPI. Cells were then trypsinized and resuspended in 500 μl medium. The numbers of total cells, GFP-positive cells, and DAPI-positive cells were measured using a Countess II FL automated cell counter with an Evos light-emitting diode (LED) cube for DAPI and GFP. The ratios of GFP-positive to DAPI-positive cells were compared between Vero cells expressing the RVFV S-GFP RNA segment [via pProK-sPI-vS(+)] and those expressing GFP mRNA (via pEGFP-N1).

Northern blot analysis. TRIzol reagent (Thermo Fisher Scientific Inc.) was used to extract RNA from Vero cells that were either mock transfected or transfected with plasmids. Denatured RNA was separated using 1% denaturing agarose-formaldehyde gels via electrophoresis. As described previously (62), Northern blots were performed using a mixture of RNA probes to detect positive- or negative-sense S, M, or L RNA segments. The pSPT18-N plasmid harbors the reverse-complementary-sense full-length N ORF (nt 39 to 776) flanked by the 5′ sequence encoding the SP6 promoter and the Hind III site and the 3' sequence encoding the Acc65I site and the T7 promoter. To generate RNA probes to detect the negative- or positive-sense S RNA segment, the pSPT18-N plasmid was linearized with HindIII or Acc65I, followed by *in vitro* transcription using T7 or SP6 RNA polymerase (digoxigenin [DIG] RNA SP6/T7 labeling kit; Millipore Sigma, St. Louis, MO), respectively. Similarly, pSPT18-M (the reverse-complementary-sense partial Gn ORF at nt 1297 to 2102 inserted between HindIII and Acc65I) or pSPT18-L (the reverse-complementary-sense partial L ORF at nt 19 to 756 inserted between HindIII and Acc65I) was used for an RNA probe detecting M or L RNA segments, respectively.

Rescue of recombinant RVFV MP-12 strain infectious clones. Vero cells in 6-well plates (1×10^6 cells/well) were transfected with 0.8 μg of pProK-sPI-vS(+), 0.8 μg of pProK-sPI-vM(+), 0.8 μg of pProK-sPI-vL(+), 0.6 μg of pCAGGSK-vN, 0.5 μg of pCAGGSK-vL, and 0.5 μg of pCAGGSK-vG using 12 μl of the TransIT-293 transfection reagent. Cells were incubated under humidified conditions with 5% CO_2 at 37°C. At 24 hpt, the culture supernatant was replaced with fresh medium. At 72 hpt, cells were trypsinized, and all cells were transferred to a 10-cm culture dish for further incubation at 37°C. To monitor the rescue of RVFV MP-12 strain infectious clones, 1 ml of the culture supernatant was collected daily from each 10-cm dish and replaced with 1 ml of fresh medium in six different wells. For the rescue of the rMP-12 strain from BHK/T7-9 cells, a subconfluent monolayer of BHK/T7-9 cells in a 6-cm dish was transfected with 2.0 μg of pProT7-vS(+), 2.0 μg of pProT7-vM(+), 2.0 μg of pProT7-vL(+), 2.0 μg of pCAGGS-vN, 1.0 μg of pCAGGS-vL, and 1.0 μg of pCAGGS-vG using 30 μl of the TransIT-293 transfection reagent. The culture supernatant was replaced with fresh medium at 24 hpt and collected at 96 hpt.

rRNA promoter sequence alignment. The precursor repetitive units of ribosomal DNA (rDNA) promoter sequences of *Homo sapiens* (chromosome 21; GenBank accession number NC_000021.9; positions 8388797 to 8389034), *Macaca mulatta* (chromosome 20; GenBank accession number NC_041773.1; positions 29808263 to 29808496), and Vero cells (GenBank accession number DI217998.1) were aligned by using CLC Genomics Workbench 7.5.5 (Qiagen Inc. USA, Germantown, MD) with the following parameters: gap open cost of 10, gap extension cost of 1, and free end gap cost.

RNA sequencing of rMP-12 stocks. Vero or MRC-5 cells were infected with Vero or MRC-5 cell passage 1 stocks with rMP-12 at a multiplicity of infection (MOI) of 0.01. Total RNA was extracted at 48 h postinfection (hpi) using RNeasy (Qiagen). Next-generation sequencing (NGS) of total RNA was performed at the Next Generation Sequencing Core Facility at UTMB. The RNA-Seq library of whole transcripts was constructed from total RNA (1.0 μg). Paired-end (75-bp) library sequencing was performed on the NextSeq 550 sequencing platform (Illumina Inc., San Diego, CA). The FASTQ files of sequence reads were quality filtered by removing reads shorter than 50 bp and adapter sequences by using CLC Genomics Workbench 7.5.5. The FASTQ reads were aligned with L, M, or S segment sequences for the RVFV MP-12 strain (GenBank accession numbers DQ375404.1, DQ380208.1, and DQ380154.1), with a similarity fraction of 0.8, a mismatch cost of 2, an insertion cost of 3, and a deletion cost of 3. Subsequently, genetic variants ($\geq$0.5%) were screened using the Basic Variant Detection tool in the CLC Genomics Workbench program, with a neighborhood radius of 5, a minimum central quality of 20, a minimum neighborhood quality of 15, and an active read direction filter. Variants ($\geq$1%) that met the criteria of a forward/reverse balance between 0.25 and 0.75, $\geq$10 independent counts, and an average quality value of $\geq$20 were then listed.

Statistical analysis. Statistical analyses were performed using GraphPad Prism 8.4.3 (GraphPad Software Inc., San Diego, CA). For comparisons among groups of GFP-expressing cells, differences were analyzed by one-way analysis of variance (ANOVA), followed by Tukey's multiple-comparison test. For comparisons among groups of viral titers, arithmetic means of $\log_{10}$ values were analyzed by one-way ANOVA, followed by Tukey's multiple-comparison test.

Ethics statement. All experiments using recombinant DNA and the RVFV MP-12 strain were performed with the approval of the Institutional Biosafety Committee at UTMB.

Data availability. The raw RNA-Seq data are available via the Sequence Read Archive (SRA) database (BioProject accession number PRJNA674398).

ACKNOWLEDGMENTS

I thank A. B. Barrett, T. L. Brasel, and D. W. C. Beasley at The University of Texas Medical Branch at Galveston (UTMB) for their helpful discussion for the RVF candidate vaccine preparation and S. Widen at the UTMB Next Generation Sequencing Core for his technical guidance and NGS support. I am also grateful to Anthony Garcia and Victoria Morris (Human Pathophysiology and Translational Medicine Program, UTMB) for their technical assistance. I also thank John C. Morrill (UTMB) for the MP-12 vaccine lot 7-2-88 and James Coffman (U.S. Army Medical Research Institute of Infectious Diseases) for the monoclonal antibody 5G2 for RVFV Gc protein.

This study was supported by NIH grant R01 AI150917-01 (T.I.) as well as generous UTMB funding support from the Department of Pathology and the Institute for Human Infection and Immunity (IHII).

REFERENCES

1. Marston HD, Folkers GK, Morens DM, Fauci AS. 2014. Emerging viral diseases: confronting threats with new technologies. Sci Transl Med 6:253ps10. https://doi.org/10.1126/scitranslmed.3009872.
2. CDC. 2007. Rift Valley fever outbreak—Kenya, November 2006-January 2007. MMWR Morb Mortal Wkly Rep 56:73–76.
3. Ikegami T, Makino S. 2011. The pathogenesis of Rift Valley fever. Viruses 3:493–519. https://doi.org/10.3390/v3050493.
4. Bird BH, Ksiazek TG, Nichol ST, Maclachlan NJ. 2009. Rift Valley fever virus. J Am Vet Med Assoc 234:883–893. https://doi.org/10.2460/javma.234.7.883.
5. Swanepoel R, Coetzer JAW. 2004. Rift Valley fever, p 1037–1070. *In* Coetzer JAW, Tustin RC (ed), Infectious diseases of livestock with special reference to southern Africa, 2nd ed. Oxford University Press, Cape Town, South Africa.
6. Phoenix I, Lokugamage N, Nishiyama S, Ikegami T. 2016. Mutational analysis of the Rift Valley fever virus glycoprotein precursor proteins for Gn protein expression. Viruses 8:151. https://doi.org/10.3390/v8060151.
7. Kreher F, Tamietti C, Gommet C, Guillemot L, Ermonval M, Failloux AB, Panthier JJ, Bouloy M, Flamand M. 2014. The Rift Valley fever accessory proteins NSm and P78/NSm-GN are distinct determinants of virus propagation in vertebrate and invertebrate hosts. Emerg Microbes Infect 3:e71. https://doi.org/10.1038/emi.2014.71.
8. Weingartl HM, Zhang S, Marszal P, McGreevy A, Burton L, Wilson WC. 2014. Rift Valley fever virus incorporates the 78 kDa glycoprotein into virions matured in mosquito C6/36 cells. PLoS One 9:e87385. https://doi.org/10.1371/journal.pone.0087385.
9. Crabtree MB, Kent Crockett RJ, Bird BH, Nichol ST, Erickson BR, Biggerstaff BJ, Horiuchi K, Miller BR. 2012. Infection and transmission of Rift Valley fever viruses lacking the NSs and/or NSm genes in mosquitoes: potential role for NSm in mosquito infection. PLoS Negl Trop Dis 6:e1639. https://doi.org/10.1371/journal.pntd.0001639.
10. Won S, Ikegami T, Peters CJ, Makino S. 2007. NSm protein of Rift Valley fever virus suppresses virus-induced apoptosis. J Virol 81:13335–13345. https://doi.org/10.1128/JVI.01238-07.
11. Terasaki K, Won S, Makino S. 2013. The C-terminal region of Rift Valley fever virus NSm protein targets the protein to the mitochondrial outer membrane and exerts antiapoptotic function. J Virol 87:676–682. https://doi.org/10.1128/JVI.02192-12.
12. Ikegami T, Narayanan K, Won S, Kamitani W, Peters CJ, Makino S. 2009. Rift Valley fever virus NSs protein promotes post-transcriptional downregulation of protein kinase PKR and inhibits eIF2alpha phosphorylation. PLoS Pathog 5:e1000287. https://doi.org/10.1371/journal.ppat.1000287.
13. Kalveram B, Lihoradova O, Ikegami T. 2011. NSs protein of Rift Valley fever virus promotes posttranslational downregulation of the TFIIH subunit p62. J Virol 85:6234–6243. https://doi.org/10.1128/JVI.02255-10.
14. Mudhasani R, Tran JP, Retterer C, Kota KP, Whitehouse CA, Bavari S. 2016. Protein kinase R degradation is essential for Rift Valley fever virus infection and is regulated by SKP1-CUL1-F-box (SCF)FBXW11-NSs E3 ligase. PLoS Pathog 12:e1005437. https://doi.org/10.1371/journal.ppat.1005437.
15. Kainulainen M, Habjan M, Hubel P, Busch L, Lau S, Colinge J, Superti-Furga G, Pichlmair A, Weber F. 2014. Virulence factor NSs of Rift Valley fever virus recruits the F-box protein FBXO3 to degrade subunit p62 of general transcription factor TFIIH. J Virol 88:3464–3473. https://doi.org/10.1128/JVI.02914-13.
16. Billecocq A, Spiegel M, Vialat P, Kohl A, Weber F, Bouloy M, Haller O. 2004. NSs protein of Rift Valley fever virus blocks interferon production by inhibiting host gene transcription. J Virol 78:9798–9806. https://doi.org/10.1128/JVI.78.18.9798-9806.2004.
17. Bouloy M, Janzen C, Vialat P, Khun H, Pavlovic J, Huerre M, Haller O. 2001. Genetic evidence for an interferon-antagonistic function of Rift Valley fever virus nonstructural protein NSs. J Virol 75:1371–1377. https://doi.org/10.1128/JVI.75.3.1371-1377.2001.
18. Grobbelaar AA, Weyer J, Leman PA, Kemp A, Paweska JT, Swanepoel R. 2011. Molecular epidemiology of Rift Valley fever virus. Emerg Infect Dis 17:2270–2276. https://doi.org/10.3201/eid1712.111035.
19. Dungu B, Lubisi BA, Ikegami T. 2018. Rift Valley fever vaccines: current and future needs. Curr Opin Virol 29:8–15. https://doi.org/10.1016/j.coviro.2018.02.001.
20. Ikegami T. 2019. Candidate vaccines for human Rift Valley fever. Expert Opin Biol Ther 19:1333–1342. https://doi.org/10.1080/14712598.2019.1662784.
21. Rusnak JM, Gibbs P, Boudreau E, Clizbe DP, Pittman P. 2011. Immunogenicity and safety of an inactivated Rift Valley fever vaccine in a 19-year study. Vaccine 29:3222–3229. https://doi.org/10.1016/j.vaccine.2011.02.037.
22. Caplen H, Peters CJ, Bishop DH. 1985. Mutagen-directed attenuation of Rift Valley fever virus as a method for vaccine development. J Gen Virol 66:2271–2277. https://doi.org/10.1099/0022-1317-66-10-2271.
23. Ikegami T. 2017. Rift Valley fever vaccines: an overview of the safety and efficacy of the live-attenuated MP-12 vaccine candidate. Expert Rev Vaccines 16:601–611. https://doi.org/10.1080/14760584.2017.1321482.
24. Pittman PR, Norris SL, Brown ES, Ranadive MV, Schibly BA, Bettinger GE, Lokugamage N, Korman L, Morrill JC, Peters CJ. 2016. Rift Valley fever MP-12 vaccine phase 2 clinical trial: safety, immunogenicity, and genetic characterization of virus isolates. Vaccine 34:523–530. https://doi.org/10.1016/j.vaccine.2015.11.078.
25. Wichgers Schreur PJ, Oreshkova N, Moormann RJ, Kortekaas J. 2014. Creation of Rift Valley fever viruses with four-segmented genomes reveals flexibility in bunyavirus genome packaging. J Virol 88:10883–10893. https://doi.org/10.1128/JVI.00961-14.
26. Bird BH, Maartens LH, Campbell S, Erasmus BJ, Erickson BR, Dodd KA, Spiropoulou CF, Cannon D, Drew CP, Knust B, McElroy AK, Khristova ML, Albarino CG, Nichol ST. 2011. Rift Valley fever virus vaccine lacking the NSs and NSm genes is safe, nonteratogenic, and confers protection from viremia, pyrexia, and abortion following challenge in adult and pregnant sheep. J Virol 85:12901–12909. https://doi.org/10.1128/JVI.06046-11.
27. Pekosz A, He B, Lamb RA. 1999. Reverse genetics of negative-strand RNA viruses: closing the circle. Proc Natl Acad Sci U S A 96:8804–8806. https://doi.org/10.1073/pnas.96.16.8804.
28. Billecocq A, Gauliard N, Le May N, Elliott RM, Flick R, Bouloy M. 2008. RNA polymerase I-mediated expression of viral RNA for the rescue of infectious virulent and avirulent Rift Valley fever viruses. Virology 378:377–384. https://doi.org/10.1016/j.virol.2008.05.033.
29. Lowen AC, Noonan C, McLees A, Elliott RM. 2004. Efficient bunyavirus rescue from cloned cDNA. Virology 330:493–500. https://doi.org/10.1016/j.virol.2004.10.009.
30. Elliott RM, Blakqori G, van Knippenberg IC, Koudriakova E, Li P, McLees A, Shi X, Szemiel AM. 2013. Establishment of a reverse genetics system for Schmallenberg virus, a newly emerged orthobunyavirus in Europe. J Gen Virol 94:851–859. https://doi.org/10.1099/vir.0.049981-0.
31. Blakqori G, Weber F. 2005. Efficient cDNA-based rescue of La Crosse

bunyaviruses expressing or lacking the nonstructural protein NSs. J Virol 79:10420–10428. https://doi.org/10.1128/JVI.79.16.10420-10428.2005.
32. Tilston-Lunel NL, Acrani GO, Randall RE, Elliott RM. 2015. Generation of recombinant Oropouche viruses lacking the nonstructural protein NSm or NSs. J Virol 90:2616–2627. https://doi.org/10.1128/JVI.02849-15.
33. Ikegami T, Won S, Peters CJ, Makino S. 2006. Rescue of infectious Rift Valley fever virus entirely from cDNA, analysis of virus lacking the NSs gene, and expression of a foreign gene. J Virol 80:2933–2940. https://doi.org/10.1128/JVI.80.6.2933-2940.2006.
34. Gerrard SR, Bird BH, Albarino CG, Nichol ST. 2007. The NSm proteins of Rift Valley fever virus are dispensable for maturation, replication and infection. Virology 359:459–465. https://doi.org/10.1016/j.virol.2006.09.035.
35. Habjan M, Penski N, Spiegel M, Weber F. 2008. T7 RNA polymerase-dependent and -independent systems for cDNA-based rescue of Rift Valley fever virus. J Gen Virol 89:2157–2166. https://doi.org/10.1099/vir.0.2008/002097-0.
36. Horaud F. 1992. Absence of viral sequences in the WHO-Vero cell bank. A collaborative study. Dev Biol Stand 76:43–46.
37. Knezevic I, Stacey G, Petricciani J, Sheets R, WHO Study Group on Cell Substrates. 2010. Evaluation of cell substrates for the production of biologicals: revision of WHO recommendations. Report of the WHO Study Group on Cell Substrates for the Production of Biologicals, 22-23 April 2009, Bethesda, USA. Biologicals 38:162–169. https://doi.org/10.1016/j.biologicals.2009.08.019.
38. Barrett PN, Mundt W, Kistner O, Howard MK. 2009. Vero cell platform in vaccine production: moving towards cell culture-based viral vaccines. Expert Rev Vaccines 8:607–618. https://doi.org/10.1586/erv.09.19.
39. Neumann G, Fujii K, Kino Y, Kawaoka Y. 2005. An improved reverse genetics system for influenza A virus generation and its implications for vaccine production. Proc Natl Acad Sci U S A 102:16825–16829. https://doi.org/10.1073/pnas.0505587102.
40. Ortiz-Riano E, Cheng BYH, de la Torre JC, Martinez-Sobrido L. 2013. Arenavirus reverse genetics for vaccine development. J Gen Virol 94:1175–1188. https://doi.org/10.1099/vir.0.051102-0.
41. Cheng BY, Ortiz-Riano E, de la Torre JC, Martinez-Sobrido L. 2013. Generation of recombinant arenavirus for vaccine development in FDA-approved Vero cells. J Vis Exp 78:e50662. https://doi.org/10.3791/50662.
42. Neumann G, Feldmann H, Watanabe S, Lukashevich I, Kawaoka Y. 2002. Reverse genetics demonstrates that proteolytic processing of the Ebola virus glycoprotein is not essential for replication in cell culture. J Virol 76:406–410. https://doi.org/10.1128/jvi.76.1.406-410.2002.
43. Song MS, Baek YH, Pascua PNQ, Kwon HI, Park SJ, Kim EH, Lim GJ, Choi YK. 2013. Establishment of Vero cell RNA polymerase I-driven reverse genetics for influenza A virus and its application for pandemic (H1N1) 2009 influenza virus vaccine production. J Gen Virol 94:1230–1235. https://doi.org/10.1099/vir.0.051284-0.
44. Tantravahi R, Miller DA, Dev VG, Miller OJ. 1976. Detection of nucleolus organizer regions in chromosomes of human, chimpanzee, gorilla, orangutan and gibbon. Chromosoma 56:15–27. https://doi.org/10.1007/BF00293725.
45. Haltiner MM, Smale ST, Tjian R. 1986. Two distinct promoter elements in the human rRNA gene identified by linker scanning mutagenesis. Mol Cell Biol 6:227–235. https://doi.org/10.1128/mcb.6.1.227.
46. Heix J, Grummt I. 1995. Species specificity of transcription by RNA polymerase I. Curr Opin Genet Dev 5:652–656. https://doi.org/10.1016/0959-437X(95)80035-2.
47. Smale ST, Tjian R. 1985. Transcription of herpes simplex virus tk sequences under the control of wild-type and mutant human RNA polymerase I promoters. Mol Cell Biol 5:352–362. https://doi.org/10.1128/mcb.5.2.352.
48. Ly HJ, Ikegami T. 2016. Rift Valley fever virus NSs protein functions and the similarity to other bunyavirus NSs proteins. Virol J 13:118. https://doi.org/10.1186/s12985-016-0573-8.
49. Wuerth JD, Weber F. 2016. Phleboviruses and the type I interferon response. Viruses 8:174. https://doi.org/10.3390/v8060174.
50. Nishiyama S, Lokugamage N, Ikegami T. 2016. The L, M, and S segments of Rift Valley fever virus MP-12 vaccine independently contribute to a temperature-sensitive phenotype. J Virol 90:3735–3744. https://doi.org/10.1128/JVI.02241-15.
51. Lokugamage N, Ikegami T. 2017. Genetic stability of Rift Valley fever virus MP-12 vaccine during serial passages in culture cells. NPJ Vaccines 2:20. https://doi.org/10.1038/s41541-017-0021-9.
52. Jordan I, Sandig V. 2014. Matrix and backstage: cellular substrates for viral vaccines. Viruses 6:1672–1700. https://doi.org/10.3390/v6041672.
53. Rodrigues AF, Soares HR, Guerreiro MR, Alves PM, Coroadinha AS. 2015. Viral vaccines and their manufacturing cell substrates: new trends and designs in modern vaccinology. Biotechnol J 10:1329–1344. https://doi.org/10.1002/biot.201400387.
54. Osada N, Kohara A, Yamaji T, Hirayama N, Kasai F, Sekizuka T, Kuroda M, Hanada K. 2014. The genome landscape of the African green monkey kidney-derived Vero cell line. DNA Res 21:673–683. https://doi.org/10.1093/dnares/dsu029.
55. Agrawal S, Ganley ARD. 2018. The conservation landscape of the human ribosomal RNA gene repeats. PLoS One 13:e0207531. https://doi.org/10.1371/journal.pone.0207531.
56. Grummt I, Maier U, Ohrlein A, Hassouna N, Bachellerie JP. 1985. Transcription of mouse rDNA terminates downstream of the 3′ end of 28S RNA and involves interaction of factors with repeated sequences in the 3′ spacer. Cell 43:801–810. https://doi.org/10.1016/0092-8674(85)90253-3.
57. Zobel A, Neumann G, Hobom G. 1993. RNA polymerase I catalysed transcription of insert viral cDNA. Nucleic Acids Res 21:3607–3614. https://doi.org/10.1093/nar/21.16.3607.
58. Morrill JC, Laughlin RC, Lokugamage N, Pugh R, Sbrana E, Weise WJ, Adams LG, Makino S, Peters CJ. 2013. Safety and immunogenicity of recombinant Rift Valley fever MP-12 vaccine candidates in sheep. Vaccine 31:559–565. https://doi.org/10.1016/j.vaccine.2012.10.118.
59. Ikegami T, Hill TE, Smith JK, Zhang L, Juelich TL, Gong B, Slack OA, Ly HJ, Lokugamage N, Freiberg AN. 2015. Rift Valley fever virus MP-12 vaccine is fully attenuated by a combination of partial attenuations in the S, M, and L segments. J Virol 89:7262–7276. https://doi.org/10.1128/JVI.00135-15.
60. Lokugamage N, Freiberg AN, Morrill JC, Ikegami T. 2012. Genetic subpopulations of Rift Valley fever virus strains ZH548 and MP-12 and recombinant MP-12 strains. J Virol 86:13566–13575. https://doi.org/10.1128/JVI.02081-12.
61. Ito N, Takayama-Ito M, Yamada K, Hosokawa J, Sugiyama M, Minamoto N. 2003. Improved recovery of rabies virus from cloned cDNA using a vaccinia virus-free reverse genetics system. Microbiol Immunol 47:613–617. https://doi.org/10.1111/j.1348-0421.2003.tb03424.x.
62. Ikegami T, Won S, Peters CJ, Makino S. 2005. Rift Valley fever virus NSs mRNA is transcribed from an incoming anti-viral-sense S RNA segment. J Virol 79:12106–12111. https://doi.org/10.1128/JVI.79.18.12106-12111.2005.
63. Won S, Ikegami T, Peters CJ, Makino S. 2006. NSm and 78-kilodalton proteins of Rift Valley fever virus are nonessential for viral replication in cell culture. J Virol 80:8274–8278. https://doi.org/10.1128/JVI.00476-06.
64. Schneider CA, Rasband WS, Eliceiri KW. 2012. NIH Image to ImageJ: 25 years of image analysis. Nat Methods 9:671–675. https://doi.org/10.1038/nmeth.2089.
65. Food and Drug Administration, Department of Health and Human Services. 2019. Code of federal regulations. Title 21. Food and drugs. Chapter I. Part 211. Current good manufacturing practice for finished pharmaceuticals. U.S. Government Publishing Office, Washington, DC.